Journal of Controlled Release 317 (2020) 154–165

Contents lists available at ScienceDirect

Journal of Controlled Release

journal homepage: www.elsevier.com/locate/jconrel

Impact of chemistry and nanoformulation parameters on cellular uptake and airway distribution of RNA oligonucleotides

Erik Oude Blenke[a], Sunny Mahakena[b], Marcel Fens[a], Joep van den Dikkenberg[a], Maarten Holkers[b], Enrico Mastrobattista[a,*]

[a] Department of Pharmaceutics, Utrecht Institute of Pharmaceutical Sciences (UIPS), Utrecht University, Universiteitsweg 99, 3584, CG, Utrecht, The Netherlands
[b] ProQR Therapeutics NV, Zernikedreef 9, 2333, CK, Leiden, The Netherlands

ARTICLE INFO

Keywords:
Oligonucleotides
Gene delivery
RNA
Nanoparticles
Local delivery
Airways

ABSTRACT

Small, synthetic oligonucleotides (ON) are of great interest as potential disease modifying drugs, mainly because of their ability to modulate previously undruggable target mutations. To date, therapeutic applications of ON are, however, limited by their physicochemical properties, including poor stability, rapid excretion and low intracellular access. In order to overcome some of these shortcomings, ON are generally formulated using nanoparticle (NP) delivery systems. Alternatively, the poor stability can be circumvented by including chemical modifications to the backbone or sugars of the ON. Some of these modifications also result in better intracellular target access of these otherwise membrane-impermeable macromolecules. Therefore, complex formulation of ON into NP in order to overcome the hurdle of intracellular access might not always be needed, especially in case of local delivery. In this study, the delivery and functionality of chemically modified ON in free form was compared to polymeric NP assisted delivery, measuring their effectivity and efficiency. For this reason, phosphorothioate (PS) backbone-modified 18-mer ON with either 2'OMe or 2'MOE-modifications were selected, capable of eliciting exon-skipping of an aberrant exon in fluorescence based *in vitro* and *in vivo* model systems. The NP consisted of poly(D,L-lactic,*co*-glycolic acid) and poly-β-amino-ester, previously demonstrated to successfully deliver nucleic acids *via* the pulmonary route. Several NP formulation parameters were tested in order to optimize the delivery of the ON, including ratio polymer:ON, NP size and concentration. The results reported here show clear differences between gymnotic and nanoparticle mediated ON delivery in terms of cellular uptake and local tissue distribution. *In vitro*, differences in exon-skipping efficiencies were observed with 2'OMe and 2'MOE ON either in free form or formulated in NP, with the striking observation that 2'OMe ON formulated in polymeric NP did not result in exon skipping. Gymnotic delivery of 2'MOE ON into the respiratory tract of mice resulted in functional delivery of exon-skipping ON into nasal epithelia and lungs as well as other downstream tissues and organs, pointing towards a gradual redistribution of locally delivered ONs, with limited but measurable systemic exposure. Conversely, NP-mediated delivery into the respiratory tract resulted in a more contained functional delivery at 10× lower ON doses compared to gymnotic delivery. Based on these findings we conclude that gymnotic delivery of 2'OMe or 2'MOE exon-skipping ON to the respiratory tract is effective, but that NP formulation might be advantageous in case spread of ON to non-target tissue can lead to undesired effects.

1. Introduction

For many pulmonary diseases harbouring a genetic underlying cause such as cystic fibrosis, COPD, asthma and ciliary dyskinesia, various types of nucleic acid treatment options have been explored, mainly because of their ability to modulate previously undruggable target mutations [1,2]. Whereas RNA-DNA-RNA hybrids named gapmers have the property to target homologous target sites in the messenger RNA, enabling RNaseH mediated degradation, RNA-based ON can engage a wide variety of mechanisms like, among others, the RNAi pathway or pre-mRNA splice-modulation. Owing to their ability to induce exon-skipping of specific exons containing mutations or the removal of pseudo-exons, many diseases are being investigated for these potent biologics. This has led to the recent FDA approval of Exondys51® (Eteplirsen) [3] and Spinraza® (Nusinersen) [4], both ON targeting their pre-mRNA targets causing exon-exclusion of exon 51 in

* Corresponding author.
E-mail address: e.mastrobattista@uu.nl (E. Mastrobattista).

https://doi.org/10.1016/j.jconrel.2019.11.025
Received 4 July 2019; Received in revised form 21 November 2019; Accepted 21 November 2019
Available online 22 November 2019

DMD or exon-inclusion of exon 7 in *SMN2*, respectively. The pulmonary route of administration for nucleic acid-based drugs is highly advantageous as it provides direct exposure to high drug concentrations in the diseased lung and prevent unnecessary exposure of non-target tissue and first-pass clearance mechanisms in case of systemic administration. For most nucleic acids, cellular uptake remains a bottleneck and for this reason they are often formulated in nanoparticles in order to aid their uptake in target cells. Interestingly, short synthetic ON with modified backbone or bases can be administered *via* the pulmonary route and reach their intracellular targets without any form of nanoparticle formulation [5,6]. It is thought that the chemical modifications to the backbone increase the stability of the ON in order for them to circulate or reside in the tissue longer, nevertheless, the precise mechanism through which they are taken up intracellularly remains unknown [5–7]. Importantly and to the best of our knowledge, to date and despite a wealth of information on the effects of chemical modifications of oligonucleotides on stability, pharmacokinetics and pharmacodynamics, surprisingly there is hardly any information how these chemical modifications influence the delivery when formulated in nanoparticles [6–8]. It is generally thought that nanoparticles enhance the delivery of ON because they protect them from degradation, but for modified ON that are already deemed stable, this advantage seems much less relevant and could be counteractive. The chemical modification of the ON could interact with compounds of the NP formulation and process, similarly the encapsulation of the ON preparation could possibly alter the cellular interaction and uptake into the cell as well as intracellular trafficking.

In order to address some of these outstanding questions, in this study, we have directly compared gymnotic *vs.* nanoparticle-mediated delivery of exon-skipping ON both on cells in culture as well as *in vivo* after local delivery into the respiratory tract elucidating some of these outstanding enquiries: i) What is the effect of the different chemical modifications of the backbone and sugars on the efficiency of splice correction? ii) Is the delivery of synthetic ON by means of nanoparticles more efficient when compared to administration without formulation? iii) Does formulation in a nanoparticle significantly change the biodistribution of these synthetic ON after delivery in the respiratory tract?

The delivery system used, is a solid polymer particle consisting of a mixture of PLGA and the cationic polymer PBAE, as previously described by Lynn and Langer [9,10]. The polymer blend of 85/15% of PLGA/PBAE was first applied in microparticles for DNA vaccination [10]. To the best of our knowledge, it was the research group led by Mark Saltzman who first adapted this to nanoparticle format and introduced an MPG peptide in order to enhance cellular uptake in non-phagocytic cells [11]. Extensive research using these NP led to the delivery of DNA/PNA molecules into the lung epithelial cells in a murine model for cystic fibrosis [12,13]. Owing to this suitability for *in vivo* lung delivery, this nanoparticle system was chosen for the delivery of chemically modified ON to induce exon-skipping.

2. Materials and methods

2.1. PBAE polymer synthesis

Poly-beta-amino esters were synthesized according to a previously described method by Lynn and Langer [9] at a 10 g scale. In brief; 1,4-butanediol diacrylate (Sigma Aldrich) (5.065 g, 25.55 mmol) and 4,4′-trimethylenedipiperidine (Sigma Aldrich) (5.375 g, 25.55 mmol) were dissolved in separate vials in 30 mL of THF. The diamine solution was added to the diacrylate solution *via* pipetting. The vial was sealed and stirred with a magnetic stirring bar, while heated at 50 °C for 48 h. After this, the reaction was cooled to room temperature and poured slowly into vigorously stirring hexane. The precipitant was re-dissolved in fresh THF and precipitated in hexane for a total of three times before collecting and drying under vacuum. The polymer was analysed by gel permeation chromatograph on a Waters Alliance 2695 Pump/injector module, with a Waters 2414 RI detector. The polymers were injected in THF on an Agilent PL Mixed-D column set at a flow of 1 mL/min and a column temperature of 30 °C. Relative molecular weights where calculated with polystyrene as a reference using Empower 3 software (Waters). Samples where dissolved in deuterated chloroform (Sigma Aldrich) at a concentration of 10 mg/mL and analysed in an Agilent 400 MHz NMR.

2.2. Nanoparticle formulation

All NP preparations were formulated containing the DSPE-PEG-MPG peptide on the outside surface. The sequence of the MPG peptide was H_2N-CGALFLGFLGAAGSTMGAWSQPKKKRKV-OH, ordered with a purity of > 95% from Genscript Inc. PLGA with intrinsic viscosity midpoints of 1.0 dL/g (PDLG5010), 0.4 dL/g (PDLG5004A) and 0.2 dL/g (PDLG5002A) were ordered from Purac Biochem, Amsterdam, the Netherlands. PLHMGA was prepared as previously described [14]. ON were ordered from Biosearch Technologies (Petaluma, CA, USA) with sequence 5′-GCTATTACCTTAACCCAG-3′. Backbone modifications were all PS and ribose modifications were either all OMe or MOE. Control ON were synthesized by GlaxoSmithKline (Stevenage, United Kingdom), sequences were 5′-CCTGUUAUACCACUUACA-3′ All PS and either all OMe or MOE. The labelled oligonucleotide was conjugated with Alexa 647 on a C6-linker 3′ of the oligonucleotide.

Nanoparticles were formulated using the double emulsion solvent evaporation method and adapted from earlier work [11]. In brief; DSPE-PEG-MPG peptide micelles were made one day before formulation. MPG peptide and DSPE-PEG-maleimide were weighed from dry powders and combined in the same vial in a 1:3 ratio. This was dissolved in MilliQ water to a concentration of 1.37 mM of peptide and rolled overnight on a rolling incubator. A blend of PLGA/PBAE in a ratio of 85/15% (wt:wt), was dissolved overnight in dichloromethane at a concentration of 10% (wt/vol). Each batch contained 80 mg of polymer (in 800 μL of DCM). To form the first emulsion, 60 μL of ON, dissolved in nuclease free water, was added dropwise and under vortexing. Feed concentrations of 'LOW', 'MID' and 'HIGH' loaded formulations were 666 μM, 6.66 mM and 33.3 mM of ON in the first aqueous phase. After vortexing the emulsion, it was sonicated on ice, for three times 10 s using a Bandelin Sonopuls HD2200 sonicator with Bandelin Sonopuls MS-37 conical tip (3 mm) at 10% intensity. The first emulsion was added dropwise and under vortexing to a second vial, containing 1.8 mL of 5% PVA (Polyvinyl alcohol MW ~30.000–70.000 Da (Sigma Aldrich)) and 15 nmol/mg of polymer DSPE-PEG-MPG micelles, which was subjected to another three times of sonicating on ice, using similar settings. This second emulsion was transferred into a stirring beaker containing 20 mL of 0.3% PVA and was left to stir for at least three hours. After the formulation was completed, the particles were transferred to a 10 mL Float-a-Lyzer G2 (1,000,000 MWCO) tube and dialyzed overnight at 4 °C in RO water. Nanoparticles were subsequently freeze dried in batches of 4 mg of polymer in Eppendorf tubes and stored at −20 °C until further use. Several nanoparticle preparations were analysed after dialysis and re-analysed after resuspension and the particle size remained similar. Furthermore, we did not observe aggregation of the preparations nor amalgamation of the particles measured by DLS.

In order to reduce particle size, emulsions were generated at lower polymer concentrations. PLGA5010 and PBAE were used in the same ratio of 85/15% (wt:wt), but weighed at 40 mg and 20 mg amounts and dissolved to 5% and 2.5% in 800 μL DCM. Aqueous volume of the first emulsion was reduced to 30 μL and 15 μL respectively to keep the ratio of aqueous phase to polymer the same.

Labelled particles for uptake studies were made with a mix of Alexa 647-labelled ON and control ON. To reduce a possible influence of the label on the formulation itself, the ratio of Alexa 647-labelled ON to polymer was kept constant. Therefore, the amount of unlabelled control ON that was used as 'filler' varied. All formulations were made with a

feed concentration of 66 μM of labelled ON.

2.3. Nanoparticle characterization

Nanoparticle size distribution was determined using Dynamic Light Scattering (DLS) and Nanoparticle Tracking Analysis (NTA). DLS was measured using a Malvern Zetasizer Nano-S (Malvern Instruments, Malvern, UK). NTA was performed using a Malvern Nanosight LM10 with a 633 nm laser and analysed with the Nanosight NTA 3.0 software. Encapsulation efficiency of labelled ON was measured indirectly from formulations made with the Alexa647-labelled ON. Formulations were spun down at 21.000 RCF for 20 min in a benchtop centrifuge instead of using dialysis tubes. The supernatant was transferred into ultracentrifuge tubes for a Beckman Coulter Optima L-90 k ultracentrifuge and spun in a Type 70.1 Ti rotor for 50 min at 100,000 RCF at 20 °C. The resulting supernatant was measured using a Jasco FP8300 Spectrofluorometer equipped with a micro-well plate reader (JASCO Benelux BV., De Meern, Netherlands). Wavelengths used were 650 nm and 665 nm. A calibration curve in 0.3% PVA was made to calculate the concentration of un-encapsulated ON.

2.4. Cell culture

The HeLa cervix carcinoma cells containing the eGFP-654 expression unit stably integrated (kindly provided by the University of North Carolina at Chapel Hill) were cultured in Dulbecco's modified Eagle's medium (DMEM) containing 1 mM sodium pyruvate and 10% fetal bovine serum (FBS) at 37 °C in a 10% CO_2 atmosphere. All media and supplements were from Sigma-Aldrich. Cells were regularly tested for mycoplasma contamination (ATCC-30-1012 K, Universal Mycoplasma Detection Kit).

2.5. Direct fluorescence microscopy

For transduction experiments, HeLa.eGFP-654 cells were seeded in a black μView clear-bottom 96.

well plate (#655090, Greiner Bio-One B.V. Alphen a/d Rijn, Netherlands) at a density of 9.0×10^3 cells/well in regular culture medium. In order to assess gymnotic uptake, oligonucleotides were diluted in OptiMEM (Sigma Aldrich) at concentrations between 20 nM and 200 μM. Nanoparticle formulations were diluted in OptiMEM to a final concentration of 5, 10, 25, 50, 75, 100, 150 and 200 μg/mL of polymer. Both types of samples were inoculated for six hours and replaced for complete medium and incubated overnight. To serve as control, HeLa.eGFP-654 cells were transfected with the ON using Lipofectamine 2000 (Thermo Fisher) according to the manufacturers protocol for (si)RNA, with a final oligonucleotide concentration of 20 nM. At the following day, the plate was imaged in a Yokogawa CellVoyager 7000S (Yokogawa, Tokyo, Japan) using confocal settings. Nuclear staining with Hoechst 33342 (Thermo Fisher) was excited with the 405 nm laser and acquired at 445/45 nm, eGFP fluorescent signal was excited at 488 nm and acquired at 525/50 nm. Alexa647 was excited at 640 nm and acquired at 676/29 nm. *Z*-offset was determined by selecting the shifting distance with the greatest intensity. The other parameters were then acquired at the same offset. Nine pictures were taken per well in four or six wells per condition. For transfection experiments, images were acquired at a magnification of 20× and for uptake at a magnification of 60×. After acquisition, pictures were analysed using Columbus software (Perkin Elmer, Groningen, the Netherlands).

2.6. Analysis of direct fluorescent microscopy images

Using the built-in "detect nuclei" function of Columbus, all nuclei in the microscope images were detected in order to create a Population. Subsequently, of this Population, the cytoplasm was detected using the eGFP fluorescence in order to create an Area. Next, intensities were calculated in the Area 'cytoplasm' for the entire Population. Based on the untransfected cells, a cut-off value was determined to select "Positive" and "Negative" cells. Of note, as there is a low level of natural occurring exon-skipping of the eGFP-654 pre-mRNA, the presence of minute fractions of eGFP-positive cells in the untransfected wells could be determined. The cut-off value was set in order to include < 2.5% of false positives in untreated wells, as previously described [15]. Results of percentage positive cells (calculated by dividing the number of eGFP-positive cells by the total number of analysed cells) are plotted in a bar graph with standard deviation in GraphPad Prism 7. A screenshot of the Analysis Sequence used in Columbus is added as Supplementary Fig. S1.

2.7. Flow cytometry

The frequencies of eGFP-positive cells in cultures transfected with ON or nanoparticles in HeLa.eGFP-654 cell cultures were determined by using a BD Canto flow cytometer (BD Biosciences). In brief; HeLa.eGFP-654 cells were seeded into 24-wells plates, at a density of 6.0×10^4 cells/well in regular culture medium. After overnight incubation, the cells were exposed to 40 μg, 80 μg or 200 μg of particles. First, the nanoparticles were dissolved in MilliQ water and subsequent dilutions were made in OptiMEM before adding the dilutions onto the cells and incubation was performed for six hours. Medium was replaced by regular culture medium and incubated at standard conditions for 72 h. In order to perform flow cytometric analysis, the transduced cells were harvested and the percentage of eGFP expressing cells of 5.0×10^4 viable single cells were analysed per experimental condition. Mock-transduced HeLa.eGFP-654 cells served to establish the cut-off between eGFP-positive and eGFP-negative cell populations. Data were analysed and plotted with the aid of GraphPad Prism 7.

2.8. Total RNA isolation

Remainders of the samples used in for the flow cytometric analysis were pelleted by means of centrifugation and total cellular RNA was isolated using the RNeasy Plus Kit (Qiagen) according manufactures guidelines. In brief; cells were lysed using RLT-buffer, and genomic DNA was removed by passing the sample through a gDNA eliminator column. The RNA was loaded into a RNeasy MinElute spin column and after washing steps, the RNA was eluted in 50 μL of RNase free water. Total RNA from animal tissues was collected again by using the Qiagen's RNeasy Plus Mini Kit, as per the manufacturer's protocol. Depending on the size of the tissue, samples were first lysed in 350–600 μL lysis buffer (freshly added 10 μL/mL β-mercaptoethanol) and homogenized using the MagnaLyser (Roche) by shaking the tissues twice for 20 s at 7000 rpm. The homogenate was immediately placed on ice before transferring into a new Eppendorf tube and centrifuged at max speed for 3 min. The resulting supernatant was handled as described above and total RNA was eluted in 50 μL of RNase free water. Concentrations were measured by using the NanoDrop Spectophotometer (NanoDrop 2000, Thermo Fisher).

In order to generate complementary DNA (cDNA), typically 100 ng of the isolated total RNA was used in a reverse transcriptase reaction using the "Maxima H Minus First Strand cDNA Synthesis Kit, with dsDNase" (Thermo Fisher Scientific) supplemented with random hexamers, dNTPs (10 mM) and Reverse Transcriptase enzyme supplied in a final reaction volume of 20 μL, according to the manufacturer's protocol. The cDNA was generated using an elongation temperature of 48 °C for 30 min and inactivated using a heat cycle of 85 °C for 15 min.

2.9. Droplet digital PCR

This cDNA was successively used to quantify the level of exon-skipping by means of a droplet digital PCR (ddPCR) assay (Biorad

Table 1
Details of the molecular assay (primers and probes) used for quantification of eGFP levels.

Name	Sequence (5′-3′)
eGFP.RNA.Fw Saz	CGTAAACGGCCACAAGTTCAGCG
eGFP.RNA.Rv Saz	GTGGTGCAGATGAACTTCAGGGTC
eGFP.RNA.FAM1	FAM-AGGGCGAGGGCGATGC-BHQ2
eGFP.RNA.HEX2	HEX-CGAGGGCGAGGGCAATAATGATACAATGT-BHQ2

QX200). For all reactions, assay mixtures were prepared containing; 10 μL of 2× ddPCR Supermix for Probes (No dUTP) (Bio-Rad, #1863023), forward and reverse primers and taqman-probes (see Table 1 below for details) diluted in MilliQ at a final concentration of 250/160 nM, respectively, in a total reaction volume of 19 μL. One microliter of a 100× diluted cDNA sample was added, mixed rigorously and used to generate droplets. Thermal cycling conditions consisted of an enzyme activation period (10 min. at 95 °C) followed by 40 cycles of a two-step thermal profile comprising of a denaturation step (30 s. at 95 °C) and a combined annealing/extension step (60 s. at 60 °C). An enzyme deactivation step (98 °C for 10 min.) was included at the end of the thermal cycling protocol before finally maintaining the temperature at 4 °C until continuation with droplet reading.

Samples were analysed with the QuantaSoft analysis software (Bio-Rad). The accepted samples were checked for both fluorophores represented by a blue (FAM) or green (HEX) colour, for species containing the aberrant exon or spliced versions, respectively. Gating based on cloud formation and fluorescence amplitude is performed automatically where possible and confirmed manually. After gating, the positive droplet count in copies/μL for the two replicates was merged with the aid of the QuantaSoft software.

2.10. Animal experiments

For this study, hemizygous BL6.eGFP-654 mice, mixed gender, 15–27 weeks at the start of the study, were used. The mice were divided equally by age and gender. The BL6.eGFP-654 mice were anesthetized using isoflurane and the formulations were administered using a micropipette in the left and right nostril, 10 μL per nostril in 5 min per dose (2 μL per min) for a total of 7 doses, administered every other day.

All mice were sacrificed 24 h after the last administration (For clarification and summary of the different groups, see Supplementary

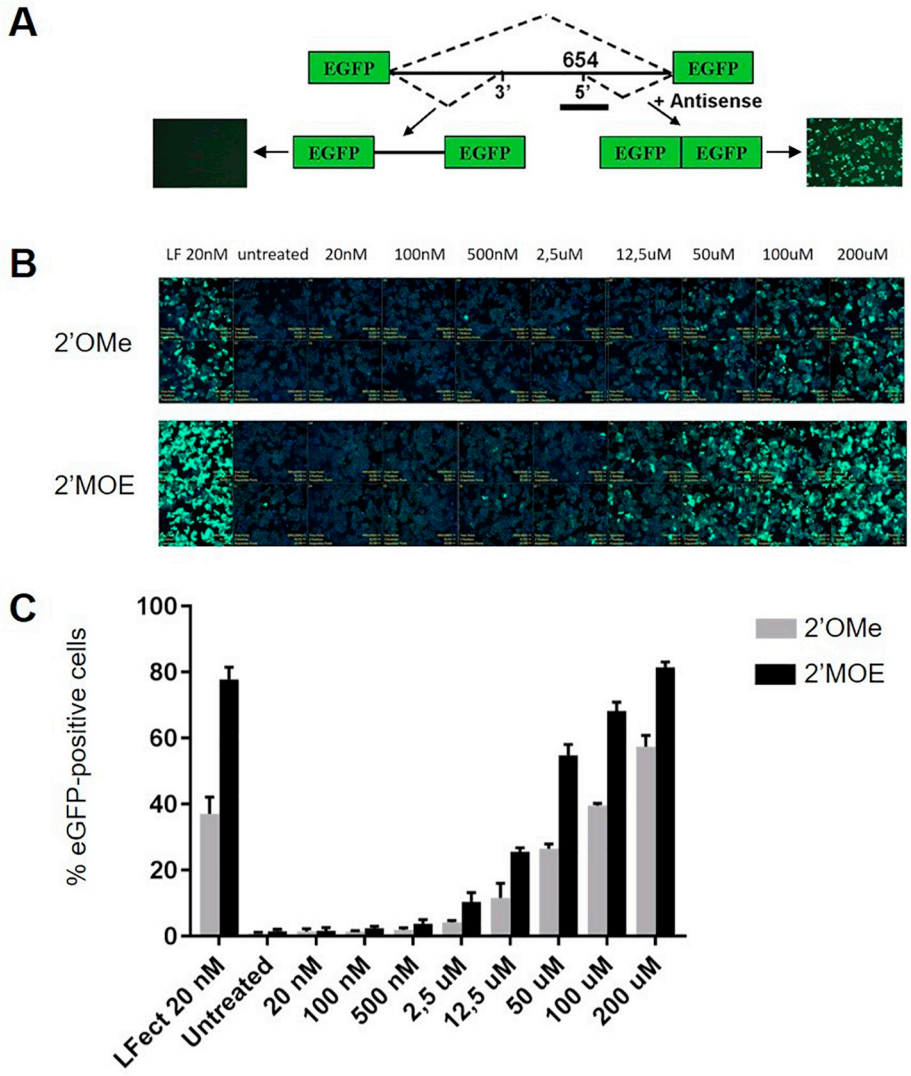

Fig. 1. RNA oligonucleotides used in this study and their potency *in vitro*.
(A) Schematic representation of the eGFP-654 expression unit. In untreated cells, the aberrant exon (654) will be included in the spliced mRNA rendering the protein non-fluorescent. When cells are exposed to the exon-skip ON (RNA 654, black bar), the sequence is skipped resulting in wild-type, fluorescent, eGFP protein. (B) Fluorescence microscope pictures of cells treated with the oligonucleotides in increasing doses. (C) Quantified data of the microscope pictures. Data is plotted as percentage of eGFP-positive cells of the total amount of cells. Mean + SD.

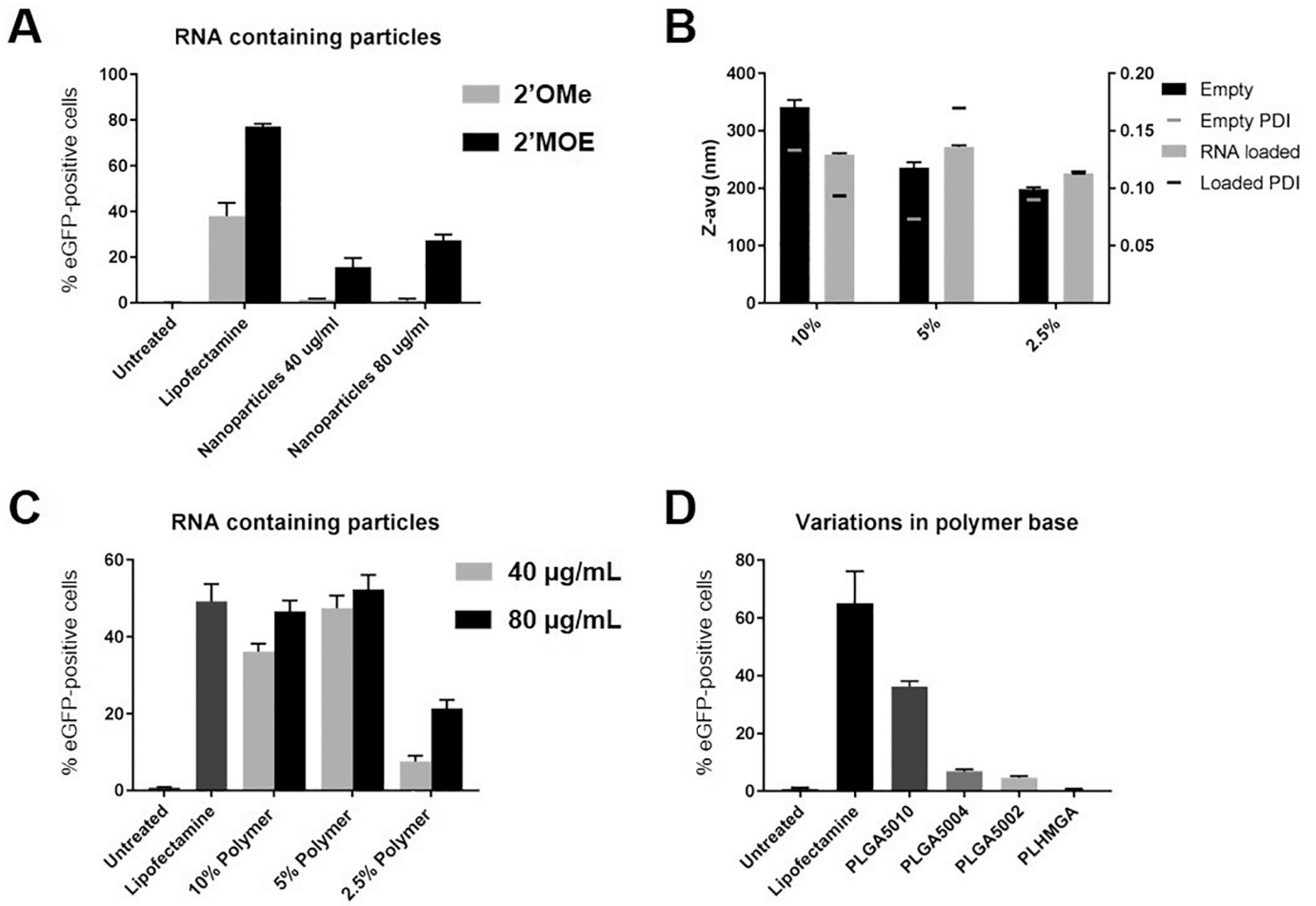

Fig. 2. Effect of variations in formulation parameters on transfection efficacy.
(A) Comparison of 2'OMe RNA with 2'MOE RNA delivery to HeLa.eGFP-654 cells when formulated in PLGA/PBAE nanoparticles. (B) Size and PDI measurements by dynamic light scattering of formulations prepared with different feed concentrations of polymer in the organic phase. (C) Effect on exon-skip using different concentrations of polymer (D) Effect on exon-skip using different polymer lengths. All data plotted as Mean + SD.

Fig. S2 and Supplementary Table S1). As a control for the 654 ON, the 705 ON was used. This is an oligonucleotide of the same length, that is complementary to a different position but will not result in altered splicing [16]. Tissues were collected for histological and molecular analysis. The following tissues were collected: nasal epithelia, trachea, oesophagus, stomach, lungs and kidneys.

2.11. Statistics

All bargraphs are plotted with data as mean + sd in GraphPad Prism 8.0.1. Statistical analysis for ddPCR data in the animal experiment was done in GraphPad Prism using ANOVA analysis with Dunnett's multiple comparisons test. Statistical significance denoted as * $p < .05$, ** $p < .01$, *** $p < .001$, **** $p < .0001$.

3. Results

3.1. Gymnotic uptake of exon skipping ON in cell cultures

Exon skipping is one of the therapeutic applications of ON and their analogues that bind to pre-mRNA in the nucleus in an antisense orientation thereby sterically blocking an RNA splice site, leading to exon exclusion. Hitherto, small synthetic anti-sense RNA oligonucleotides (AON) directed to the splice-site have been used and recently, Exondys51® (Eteplirsen) [3] and Spinraza® (Nusinersen) [4], both ON targeting their pre-mRNA targets causing exon-exclusion of exon 51 in *DMD* or exon-inclusion of exon 7 in *SMN2*, respectively, were approved by the FDA as the first disease modifying drug available.

For this study, we decided to use a model system previously described to be amendable for exon-skip studies [15]. In this system, an exogenous eGFP expression unit, containing an aberrant intronic region derived from the human β-globin IVS 654 mutation is integrated in HeLa cells and in the genome of Bl6.eGFP-654 mice. In untreated cells, the aberrant exon will be spliced in and the resulting translated mRNA will generate a non-fluorescent protein whereas, after treatment with the RNA-654 ON, wild-type eGFP sequences will result in fluorescent protein (Fig. 1A). Furthermore, we used ON containing the two most commonly employed chemical modifications to the sugar moiety described in literature; 2'methoxyethyl (2'MOE) and 2'O-Methyl (2'OMe). To determine if nanoparticle formulation results in enhanced delivery of these ON, we first measured the basic level of exon-skip after gymnotic uptake of the ON in cell cultures. Cell cultures exposed to increasing amounts of ON (ranging from 20 nM up to 200 µM) displayed an increase in eGFP-positive signal, visualized after 24 h and displayed in Fig. 1B.

Quantification of the eGFP signal by means of counting the fluorescence intensities of eGFP-positive cells revealed an increase of the fluorescent signal with increasing ON concentrations in the medium. The samples exposed to ON containing the 2'MOE modification outperformed their 2'OMe counterparts in all concentrations, reaching a similar level of eGFP-positive cells with a ~4-times lower concentration of molecules (Fig. 1C). Moreover, the use of a transfection reagent

(Lipofectamine 2000, LFect) serving as a positive control for cellular uptake and function, also displayed a difference between the two entities. It remains unclear whether the difference in the number of eGFP-positive cells after exposure to the two different types of chemically modified ON is merely the effect of the chemical modification or that it is caused by differences in complex formation, membrane passing or endosomal release. Nevertheless, both preparations were able to engage with the transcribed pre-mRNA and mediate exon-skipping, which resulted in up to 82% eGFP-positive cells.

3.2. Nanoparticle-mediated delivery of ON

Exposure of ON to cells in culture does result in the uptake and function of these molecules, nevertheless, the concentrations used are 5000-fold higher compared to those used in forced transfection protocols and such high concentrations might be prohibitive in terms of manufacturability and toxicity in a clinical setting. In order to reduce these amounts and to increase the transfection efficacy, ON can be formulated into nanoparticles. These particles have been shown to display similar transfection efficacy compared to those reached by means of transfection reagents, without causing significant cytotoxicity.

Based on the extensive pre-clinical investigation of the PLGA/PBAE polymeric nanoparticles by the research group of Saltzman, we have chosen this method to formulate the ON [12,13,17–21]. However, none of their publications contained RNA-based ON nor the chemical modifications used in the selected ON. Therefore, we first generated PLGA/PBAE nanoparticles with the formulation procedure published here [12,13] containing the 2′OMe and 2′MOE RNA ON and incubated HeLa.eGFP-654 [15] cell cultures with two concentrations of these batches in order to determine if these nanoparticles would be suited for our purposes.

Surprisingly, when cells where exposed to nanoparticles containing the 2′Me-modified ON, it failed to produce any eGFP-positive cells above the threshold set by non-transfected cell cultures (Fig. 2A). Conversely, the batches containing the 2′MOE-modified ON did so in a concentration dependent manner. A Lipofectamine™ transfection protocol using the two different ON showed the same pattern as depicted in Fig. 1C (left bars). Different batches and preparations of 2′OMe ON nanoparticles were tested but all failed to induce exon skipping. Therefore, from this point forward, we omitted the 2′OMe-modified ON in further experiments.

3.3. Nanoparticle characterization

The nanoparticles used in the previous experiments had an average size around 250 nm. For optimal penetration in de deeper layers of the lung, smaller particle size is to be preferred. Therefore, we set out to investigate whether the formulation protocol could be adapted resulting in nanoparticles with reduced size but still able to deliver functional ON. The first change was to increase the sonication times and power intensity. As these particles are generated using a double emulsion preparation method by tip sonication, increasing the sonication time and power parameters could lead to a reduction in droplet size and thereby reduction in nanoparticle size. However, this turned out not to be the case, suggesting that the size of the emulsification droplets was dictated by surface tension and viscosity of the two phases (data not shown). Therefore, the polymer concentration was lowered, to reduce the viscosity of the organic phase. Theoretically, lowering the viscosity should lead to smaller organic droplets in the w/o/w emulsion, which determines the diameter of the particles. Next to the 10% of polymer concentration used in the standard protocol, 5% and 2.5% of total polymer in DCM were tested.

Indeed, when the percentage of total polymer was reduced in preparations without oligonucleotide cargo, the average size of the particles was reduced, supporting our hypothesis on viscosity (Fig. 2B; black bars). It was observed that the solution containing 10% polymer was more viscous compared to the solution containing 2.5% polymer. The polydispersity of the particles was measured and depicted in Fig. 2B. During rigorous vortexing, the former created air pockets while the latter did not. Nonetheless, when a cargo was added to the mixtures, consisting of a negatively charged oligonucleotide, there were no differences in particle size (Fig. 2B; grey bars). We assume that, in solution, these molecules will be localized at the surfaces between the two phases and influence the droplet size and therefore the diameter of the particles generated.

After measuring nanoparticle characteristics of these different preparations, we used them to transfect cell cultures with two different concentrations of nanoparticles to assess their transfection efficacy. Strikingly, while the nanoparticles formulated using the 10% and 5% total polymer concentration demonstrated similar efficacies as described above, the batch generated using the 2.5% polymer had a much-reduced transfection efficacy (Fig. 2C). As these batches were all generated using the same amount of ON, the only measurable difference is the average particle size (260 nm and 270 nm for the 10% and 5% solutions, respectively compared to 225 nm for the 2.5% polymer batch. (See Table S2). It seems unlikely that this big decrease in performance is caused only by the seemingly small decrease in particle size. So further investigation is necessary to pinpoint the exact reason for the observed differences, like particle loading, charge and particle integrity.

3.4. Transfection efficacy of particles with different polymer bases

Besides the polymer concentration, another factor that could influence the viscosity of the organic phase solution is the molecular weight of the polymer itself. The PBAE used in the formulations has a molecular weight of ~15 kDa, conversely, the molecular weight of the PLGA, that forms the bulk of the polymer matrix, can be varied. In the previously described experiments, we have used PLGA with a molecular weight of ~110 kDa which has a more dominant effect on the viscosity of the solution and thereby particle size.

Therefore, we formulated batches of nanoparticles using PLGA with dissimilar molecular weights, keeping the molecular weight of the PBAE constant as well as the ratio of the two polymers. The polymer bases that we used were PDLG5010 of ~110 kDa, PDLG5004 of ~40 kDa, PDLG5002 of ~20 kDa and PLHMGA with a mass of ~15 kDa. PLHMGA is an in-house synthesized polymer that contains hydroxymethyl-glycolic acid next to lactic acid in order to make it more hydrophilic, which could make it more compatible with the oligonucleotide cargo [14,22].

All formulations were generated with 10% total polymer concentration in DCM. The different batches of PLGA had a clear effect on the viscosity of the solutions, most likely owing to their differences in lengths of the polymer chains. The particle size showed a trend towards smaller particles for shorter PLGA polymer lengths, with the smallest being the preparation generated using the PLHMGA polymer, as expected (Table 2), which is most likely being explained by the lower viscosity of the solutions, allowing the emulsification of smaller droplets.

It was hypothesized that similar polymer chain length of the PBAE and PLHMGA would favour polymer blending and therefore formation of more homogeneous particles. However, when these preparations were used in a transfection protocol of cell cultures, the original PDLG5010 batch outperformed the ones made with PLGA of lower molecular weights, whereas the PLHMGA formulated nanoparticles failed to result in any eGFP-positive cells above the background set by non-transfected cells (Fig. 2D).

All the experiments and preparations above clearly demonstrate the robustness of the original nanoparticle formulation protocol using the 2′MOE chemically modified oligonucleotide. Changing the total polymer concentration or the molecular weight of the PLGA polymer did not result in an enhanced transfection efficacy. As we measured the

Table 2
Effect on PLGA chain length on particle size.

Polymer base	*Z*-avg (nm)	PDI	Number mean (nm)	HWHM[a]	Volume mean (nm)	HWHM[a]	Intensity mean (nm)	HWHM[a]
PDLG5010	283	0,10	235	73	305	97	293	83
PDLG5004	252	0,03	196	71	286	111	278	94
PDLG5002	244	0,09	175	70	279	119	275	100
PLHMGA	174	0,08	140	37	171	86	202	81

[a] HWHM: Half width at half maximum.

complexation of the particles and cargo of all the different formulations using a labelled control oligonucleotide in parallel, reducing the particle size does not result in less ON per amount of polymer (Supplementary Table S3). In conclusion, the polymer concentration (10%) and high molecular weight of the PLGA (PDLG5010) described in the original protocol performed the best in terms of transfection efficacy and delivery of 2'MOE modified ON to cultured cells.

3.5. Effect of higher loading on transfection efficacy

The encapsulation efficiency of 2′MOE ON was calculated by making use of an Alexa 647-labelled ON. Notably, the encapsulation or complexation of the ON was consistently nearing 100%, even when the particle size became increasingly smaller (see Supplementary Table S3 for an overview). This observation indicates that loading efficiencies (relative weight ratio ON to polymer) have not yet reached their maximum. Therefore, to increase the oligonucleotide cargo per particle, the feed concentration of ON in the inner aqueous phase of the emulsion was increased. For nomenclature, from this point on, we used the designation 'LOW' for the original oligonucleotide concentration, 'MID' for a 10× higher concentration and 'HIGH' for a 50× higher concentration compared to the 'LOW' prepared at a constant polymer concentration. This corresponded to RNA/polymer ratios of 0.5 nmol/mg, 5 nmol/mg and 25 nmol/mg respectively. Surprisingly, it was found that all ON were associated with the nanoparticles and, even at the 'HIGH' RNA/polymer ratio, none of ON were left 'un-encapsulated' or 'non-complexed' (Supplementary Table S3).

As we hypothesized that the increase in cargo-load would directly result in an increased eGFP-positive cell count after transfection of cell cultures, nanoparticles were dosed in ranges of 5–200 μg/mL of polymer, for the three RNA loading concentrations as described above instead of the previously used 40 and 80 μg/mL. Results of the different transfections are plotted in Fig. 3 now with nanomolar concentrations on the x-axis. For the 'LOW' and 'MID' nanoparticle batches, there is a dose-dependent effect in the low concentrations. The number of eGFP-positive cells reached a plateau at 25 nM for the 'LOW' preparation whereas the 'MID' batch reached the maximum percentage of eGFP-positive cells only at 125 nM. Because the 'MID' nanoparticle formulation has a 10× higher RNA/polymer ratio, this means that to achieve the same effect, the 'MID' formulation requires a 2-fold higher amount of polymer. Obviously, with the higher doses of polymer the 'MID' formulations also achieve a higher effect, but this is solely due to the higher amounts of RNA in these formulations. This indicates that the amount of (cationic) polymer per RNA molecule is an important determinant of success. Furthermore, this means that the number of NPs added to the cells and not the absolute amount of ON determines the exon skipping efficacy. We have seen similar results in the past with nanoparticles for pDNA delivery [23]. In line with this, the transfection efficacy is almost completely abolished for the 'HIGH' nanoparticle preparation where even less polymer is available per RNA molecule. With these particles only the higher concentrations in the *in vitro* transfection media produced numbers of eGFP-positive cells above the threshold. So, in terms of efficiency and cost of goods there is in fact a clear advantage of the 'LOW' RNA/polymer ratio. When comparing this most efficient formulation to free oligonucleotides, the dose of RNA could be lowered 2000-fold (See Fig. 1C. a dose of 50 μM free MOE oligonucleotide achieves roughly the same result as the 25 nM formulated in the 'LOW' nanoparticles).

However, when the goal is to deliver as much RNA as possible, the 'HIGH' particles could have an advantage, for example when injection/administration volumes are low, like in an animal experiment.

3.6. Localized effect after delivery of nanoparticles to the airways of mice

Being able to translate experimental results using an *in vitro* model-system into a complex *in vivo* model-system with the exact same biological read-out has many benefits. Importantly, in the case of ON, sequence specificity and pre-mRNA splicing sequence context can vary between species. When a lead candidate is ready to proceed into murine models for efficacy and safety studies, these subtle differences can create dissimilar results. Here, in order to examine the efficiency of delivery, we made us of the exogenous reporter gene construct based on wild-type eGFP expression initiated by oligonucleotide-mediated exon-skipping [15]. The availability of the Bl6.eGFP-654 murine model system [6] would, theoretically, enable us to use histology combined with direct fluorescent microscopy to determine the effect on murine tissues after treatment with the ON. Nonetheless, due to the high intrinsic auto-fluorescent properties of tissue material, presumed to originate from endogenous cellular protein content, we used a ddPCR quantification method measuring the different mRNA isoforms in tissue homogenates. This method can discriminate between mRNA fragments containing the aberrant exon and fragments with the wild type eGFP sequence by means of fluorescent probes.

'Free' ON and the 3 types of nanoparticle preparations described above were used to dose the BL6.eGFP-654 mice into the respiratory tract using intranasal administration in a previously published dosing regimen [12]. All parts of the upper airways (nasal epithelium, trachea and lungs) were analysed individually, as well as off-target organs (kidney) addressing the systemic exposure after intranasal dosing. Next to these organs, the oesophagus and stomach were isolated serving as an indicator for secondary exposure. In order to set the baseline for delivery of functional ON, 'free' ON were dosed according to the regimen depicted in Supplementary Fig. S1. After sacrificing the animals, tissues were collected, total RNA was isolated and subjected to the ddPCR protocol capable of discriminating between the two isoforms of eGFP mRNA fragments. Control ON capable of binding the eGFP mRNA without causing exon-skip were taken along as well as non-treated animals. As expected, the 'free' 2'MOE-654 ON induced exon-skipping of the aberrant exon in the eGFP expression system. In nasal epithelial samples dosed with 5 nmol of 2'MOE ON roughly 2.5% of the total eGFP mRNA did contain the wild-type sequence compared to the mock treated samples which contained 0.6% of naturally skipped eGFP-sequences (Fig. 4A). Strikingly, when the highest dose of 35 nmol was used, the levels reached almost 50% of wild-type eGFP sequences, demonstrating the potential of gymnotic delivery of chemically modified ON for exon-skipping in the airways. These levels were increasingly lower when the tissue of downstream organs, trachea (Fig. 4C) and lungs (Fig. 4B) were examined, nevertheless, the high dose of 'free' ON significantly increased the levels above the background in these samples. Control samples (oesophagus [Fig. 4F] and kidney [Fig. 4D]) did

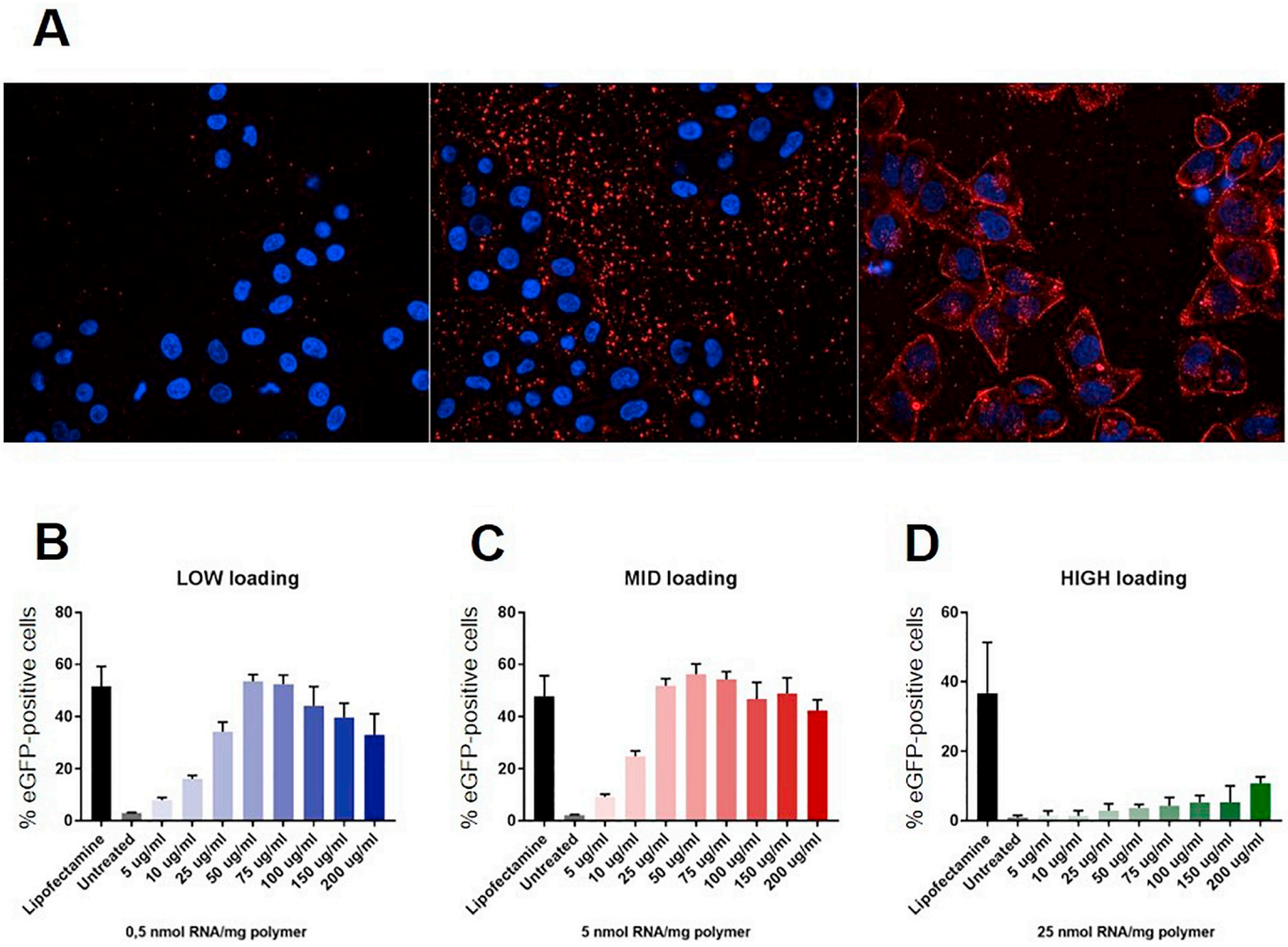

Fig. 3. Uptake and transfection efficacy of nanoparticle formulations with varying RNA/polymer ratios.
(A) Fluorescent microscopy pictures of cells transduced using formulations with increasing concentrations of oligonucleotide to polymer. In blue; Hoechst-staining of cell nucleus. In red; fluorescently labelled oligonucleotide (B-D) Percentage of exon-skip after transduction of HeLa.eGFP-654 cells with nanoparticles produced using different concentrations of oligonucleotide to polymer. The concentration of oligonucleotide per transduction is listed in nM. Data as Mean + SD. (For interpretation of the references to colour in this figure legend, the reader is referred to the web version of this article.)

show elevated levels suggesting secondary exposure and systemic exposure to tissues in the treated animals, respectively.

The rationale behind the 5 nmol and 35 nmol concentration was deduced from the nanoparticle formulation, where, assuming a 100% encapsulation efficiency, 0.5 nmol of ON were dosed in the 'LOW' nanoparticle batch, 5 nmol in the 'MID' NP batch, 25 nmol in the 'HIGH' NP preparations. Animals treated with the nanoparticle batches did not show any discomfort and behaved similar as mock-treated animals. Tissue samples were collected similarly to the 'free' ON treated animals and total RNA was isolated. In all cohorts treated with the nanoparticle formulations, clear increase in the levels of skipped eGFP mRNA was detected, with the 'LOW' and 'MID' formulations outperforming the 5 nmol 'free' oligonucleotide counterpart (Fig. 4A). The 'HIGH' nanoparticle formulation, which failed to produce elevated eGFP-positive cells in *in vitro*, showed levels up to 8.0% of skipped eGFP mRNA in nasal epithelial tissue samples as well as elevated levels in the lung tissue (Fig. 4A, B). This exon skipping pattern observed with the 'HIGH' NPs is comparable to that of free ON, albeit at lower exon skipping efficiencies, which hints towards premature release of the ON from the 'HIGH' NP. Non-target exposure (Fig. 4E and F), as well as systemic exposure (Fig. 4D), was not significantly elevated in samples derived from mice treated with all NP formulations, suggesting targeting and reduced off-target exposure. In all cases, the control oligonucleotide treatment, both 'free' as well as formulated in nanoparticles, did not show any elevated levels of eGFP mRNA exon skip, highlighting the specificity of the targeting oligonucleotide sequences.

4. Discussion

In this study, we sought out to directly compare gymnotic delivery of chemically modified ON capable of provoking exon-skipping with NP-assisted delivery in an *in vitro* model system as well as in mice after local delivery to the respiratory tract. First, we started by systematically analysing the use of different formulation parameters on the ability of NP to deliver ON into cell cultures compared to gymnotic delivery. As starting point, we transfected reporter cell lines with two different preparations of RNA-based ON, stabilized by chemical modification of the backbone (phosphorothioate) and 2'sugar moiety (2′OMe or 2′MOE). For quantification, we made use of a high throughput screening microscope and automated image analysis, whereby the direct fluorescent microscopy pictures (Fig. 1B) are used to quantify the eGFP-positive cells (Fig. 1C). The exact analysis sequence in Columbus software is added to the Supplementary Figures (Fig. S1). Simultaneously, from the pictures in Fig. 1B, it can be appreciated that the number of green cells coincides with an increase in the intensity of the fluorescent signal intensity.

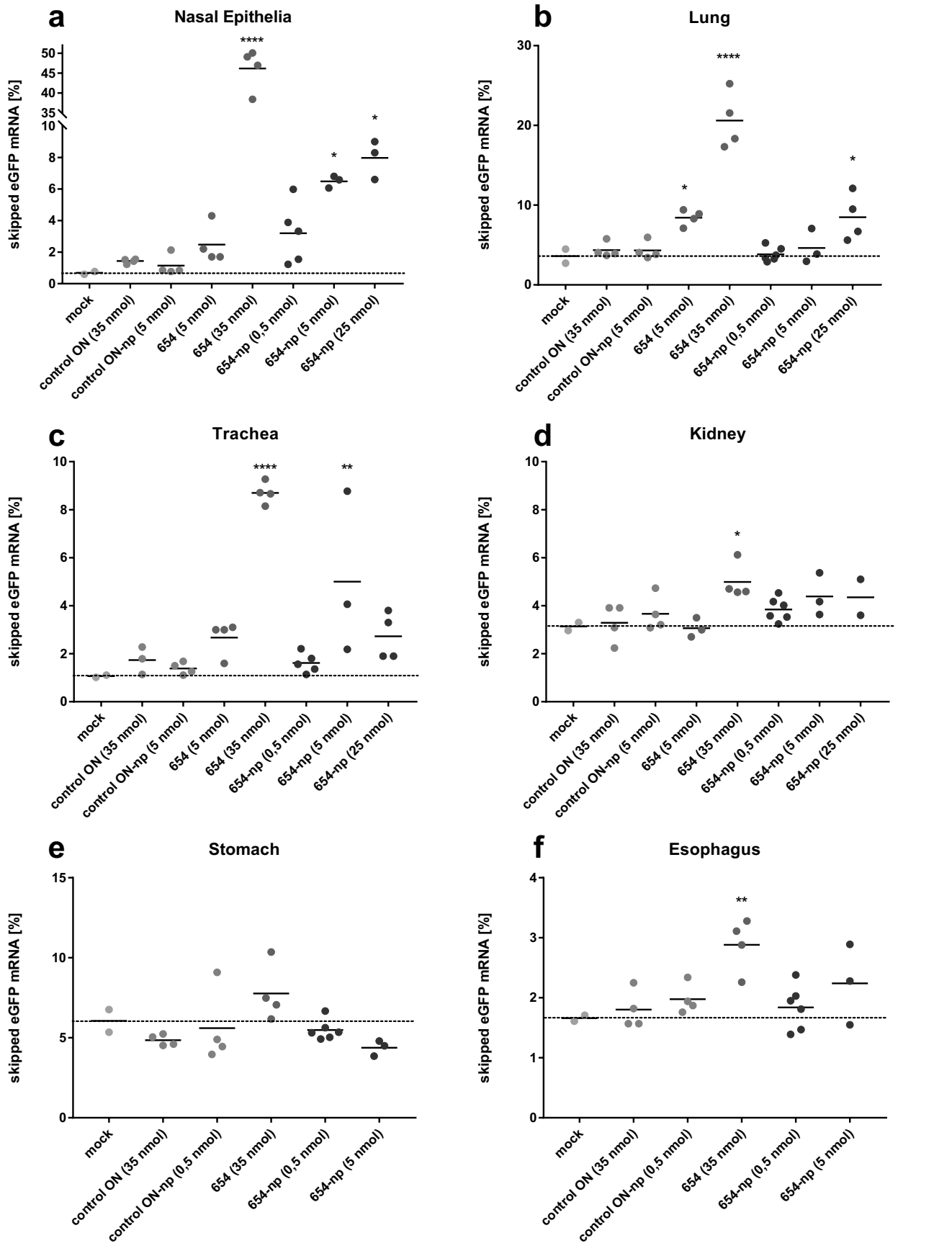

(caption on next page)

Fig. 4. *In vivo* skipped eGFP mRNA as measured by ddPCR in various on- and off-target tissues.
Free RNA ON and ON formulated in nanoparticles (np) are dosed intranasally to mice. In the case of particles, 1 mg of polymer is dosed, x-axis denotes the varying doses of ON. In the nasal epithelia there is a clear effect of increasing doses of RNA per particle on the percentage of skipped (corrected) eGFP mRNA. In this tissue, to which the bolus was dosed, the 0.5 nmol dose of ON in nanoparticles performs better than the 5 nmol dose of free ON, demonstrating a preference for formulated ON. Note that in this graph, the 35 nmol dose of free ON produced > 15% of skipped mRNA and is therefore outside the range of the y-axis. In all other tissues this extremely high dose of free ON also produced the highest percentage of skipped mRNA, including in all the off-target tissues (kidney, stomach, and oesophagus). * denotes $p < .05$, ** $p < .01$, **** $p < .0001$.

With the basal level of transfection using the 'free' ON conditions determined, we deployed the nanoparticle formulation previously described by the research group of Saltzman [12,13] and tried to change different formulation parameters in order to enhance the delivery of functional ON. Surprisingly, the chemical modifications of the ON themselves already made a difference as the 2′OMe modified versions failed to result in exon-skipping of the expressed eGFP reporter gene. Conversely, the 2′MOE modified ON did demonstrate its ability of induce exon-skipping of the aberrant exon in the eGFP pre-mRNA. The lack of wild-type eGFP transcripts after treatment with 2′OMe modified was observed in several experiments, different ON batches and using multiple separate formulations ruling out technical problems in the NP generation or ON synthesis. The main difference between these two molecules is the modification of the 2′ sugar moiety, which is bulkier in the 2′MOE form. Another difference is the 5′Methyl-C which is related to the synthesis methodology of the 2′MOE modified amidites and is linked to lowering the proinflammatory effect of ON, which is lacking in the 2′OMe containing ON. It would be interesting to know if unmodified RNA or mix-mers of both modifications behaves similarly to either one of the modified versions, which might shed light on the reason behind this difference. As the chemical characteristics and loading efficiency of the NP themselves didn't change, it hints towards a difference in release upon internalization.

Particle sizes reported in the studies performed by Saltzman et al. were large (200-300 nm). This does not necessarily pose a problem for respiratory administration (as opposed to intravenous injection), nevertheless, it could hamper the uptake in target cells [24,25]. Therefore, it was attempted to alter the formulation method in order to produce smaller particles. It was found that changing sonication settings had little effect on the particle size. Reducing the nanoparticle size by means of reducing the viscosity and surface tension in the W/O/W emulsions using PLGA polymers of different lengths or by decreasing the concentration during formulation did not correlate with an enhanced transfection efficacy. In fact, the correlation was inverted. During the formulation, the encapsulation efficiency was determined to be close to 100% in all cases, decreasing the likelihood that the reduced size would correlate with a reduction in the total amount of ON packaged. Nevertheless, the transfection efficacies of the tested nanoparticle formulation where always outperformed by the original nanoparticle recipe. Since the encapsulation efficiency was close to 100% in the nanoparticle formulations tested, we tried to increase the ON cargo 10 and 50-fold. The nanoparticle preparations with a 10-fold increased cargo did increase the percentage eGFP-fluorescent cells combined with a higher mean fluorescent intensity suggesting that these particles were able to deliver more ON into the transduced cells. Conversely, increasing the load 50-fold compared to the original recipe completely abolished functional delivery. Despite we could not measure the zeta potential of these NP, we believe that loading of the NPs with high amounts of ON leads to change in surface charge and thereby change in how these NPs interact with the cells. Indeed, fluorescence microscopy showed a completely different uptake pattern with the NPs loaded with high amounts of ON as compared to those with low or medium loading (Fig. 3A).

Finally, in order to translate the results obtained from the *in vitro* reporter system to an *in vivo* model system containing the similar reporter cassette, nanoparticle formulations were investigated by intranasal administration in BL6.eGFP-654 mice. With this administration route, nasal epithelium, trachea and lungs are considered target tissues and all other analysed tissues as off-target tissues, that indicate ingestion of the dose (oesophagus, stomach) and/or systemic absorption (kidney). After serial administration, tissues were collected, and isolated RNA was subjected to a ddPCR protocol. In all isolated tissue homogenates derived from mice that were treated with 'free' ON, ON mediated exon-skip of the aberrant exon was detected in both dose groups. In the lowest concentration (5 nmol), the rate of exon-skip was only significantly increased in the lung, but in none of the off-target tissues. For the high dose of 'free' ON (35 nmol) significant increases of exon-skip were seen in all target tissues, most notably in nasal epithelium and lung but exon-skipping also occurred in the off-target tissues oesophagus and kidney. An equally high dose of a control ON did not lead to any significant exon skipping in any tissue. The kidney exposure after administration of the 35 nmol dose suggests that this dose of 'free' ON also leads to undesired systemic absorption, which could have occurred either *via* the lung or *via* the intestinal tract. Interestingly, exon-skip rates in the stomach were not statistically significant for any of the treatment groups but it is not clear whether this is due to sample size or that the observed systemic absorption was through other tissues that had a higher exposure to the dose.

At the site of administration, the nasal epithelium, levels above 50% of exon-skipped eGFP mRNA were detected, which raised the question whether this is a feasible number in all target tissues. Immunohistochemistry of the nasal epithelium demonstrates that there are multiple cell layers making up this tissue (estimated to be up to 10 cell layers) [26]. If only the exterior layer of the tissue is exposed to the ON, only a maximum of 10% can be reached when the whole tissue is processed. This even assumes 100% exon-skipping efficiency and although these estimations are purely hypothetical, the measured 50% is so high that it suggests penetration of the ON into the deeper tissues, which can be considered as off-target and could lead to systemic exposure as well.

Deploying three different nanoparticle formulations containing 0.5, 5 nmol or 25 nmol of ON per dose, similar levels of exon-skip can be detected in the target tissues with no off-target effects at all, in any of the tissues. The 5 nmol of nanoparticle formulated ON resulted in a significant increase in exon-skip in the nasal epithelium and an additional increase was observed in the 25 nmol dose group, although that additional effect was moderate compared to the increase in dose. So, in the nasal epithelium where the dose was deposited, a clear advantage was demonstrated for ON formulated in nanoparticles over the 'free' ON. However, downstream tissues demonstrated an inversed pattern, whereby the lungs, which can be the depot of inhaled material, clearly have more exon-skipped eGFP mRNA in the 'free' ON samples. These differences suggest specific targeting to cells in the nasal epithelial tissue and reduced 'leakiness' to secondary exposed tissues. Of note, the peptide used on the nanoparticles is not specific to a receptor solely exposed on target cells, which, when changed to a targeting moiety, could enhance the tissue specificity even more.

The groups treated with nanoparticle formulations all received a dose of 1 mg of polymer per occasion, but with increasing doses of ON in the same number of particles. Strikingly, although this did not produce eGFP-positive cells in the *in vitro* model system, a clear increase in exon-skipped eGFP mRNA was detected in nasal epithelial, trachea and lung tissue samples without significant secondary (oesophagus and stomach) nor systemic (kidney) exposure. At the same time, although a

2000-fold dose reduction for formulated ON *vs.* 'free' ON was shown *in vitro*, this advantage was much less pronounced *in vivo*, even in the nasal epithelium that had the highest exposure. This indicates that nanoparticle formulation influences the distribution and localization of the ON much more than it increases cellular uptake. In a therapeutic setting, this could be exploited to achieve high local concentrations with a relatively low dose and to limit off-target and systemic exposure that are associated with high dosing.

5. Conclusions

The results presented here demonstrate that PLGA/PBAE nanoparticles can be used for functional delivery of exon-skipping ON to the respiratory tract, although further research is needed to see the efficacy in mouse models of lung disease in which additional barriers will hamper functional delivery to the lung epithelial cells. NP-assisted delivery of 2′MOE ON to reporter cells in culture was effective at doses that were 2000-fold lower than gymnotic delivery. Strikingly, 2′OMe ON lost their activity when formulated in PLGA/PBAE NPs for reasons that remain unclear. *In vivo*, the differences in exon-skipping efficacy between gymnotic and NP-assisted delivery were not that pronounced. However, NP-assisted ON delivery resulted in a better retention of the ON in the respiratory tract with exon skipping restricted to the airway tissues and no detectable levels of exon-skipping in off-target tissues such as oesophagus, stomach and kidneys. Although ONs were delivered locally to the respiratory tract and taken up by the cells *via* gymnosis, exon skipping in non-target kidney tissue was detected, albeit at very low levels. These measurements suggest that free ON can reach the circulation and result in systemic exposure, to initially untargeted tissues, and can be cleared from the system *via* the kidneys.

The choice for gymnotic or NP delivery for ON treatment of lung diseases is dependent on many factors, including degree of tissue penetration, efficiency in intracellular delivery, toxic side effects as well as pharmacoeconomic factors. NP formulation and industrial manufacturing is complex and costly, but this increase in costs might be compensated by the gain in reduced ON dose needed for effective treatment. If targeted delivery is essential due to potentially toxic effects of ON to non-target tissue, the use of NP is to be preferred as the results in this study clearly showed a more contained delivery of exon-skipping ON with NP as compared to gymnosis. However, due to their size, it is expected that nanoparticles will have more difficulty in penetrating mucous layers as compared to free ON. Another mode of delivery that combines both gymnotic and particle-assisted delivery would be the use of nano- or microparticles to deposit ON into the lungs where they can provide sustained release of therapeutic ON for prolonged treatment of chronic inflammatory lung diseases. Further research is needed to prove feasibility of such a mode of delivery.

Declaration of Competing Interest

This work was partially funded by ProQR Therapeutics NV. Funding included salary costs of Erik Oude Blenke and bench fees. Erik Oude Blenke is currently employed at AstraZeneca, Gothenburg. AstraZeneca was not involved in the conception or execution of the research described in this manuscript.

Appendix A. Supplementary data

Supplementary data to this article can be found online at https://doi.org/10.1016/j.jconrel.2019.11.025.

References

[1] E.W.F.W. Alton, D.K. Armstrong, D. Ashby, K.J. Bayfield, D. Bilton, E.V. Bloomfield, A.C. Boyd, J. Brand, R. Buchan, R. Calcedo, P. Carvelli, M. Chan, S.H. Cheng, D.D.S. Collie, S. Cunningham, H.E. Davidson, G. Davies, J.C. Davies, L.A. Davies, M.H. Dewar, A. Doherty, J. Donovan, N.S. Dwyer, H.I. Elgmati, R.F. Featherstone, J. Gavino, S. Gea-Sorli, D.M. Geddes, J.S.R. Gibson, D.R. Gill, A.P. Greening, U. Griesenbach, D.M. Hansell, K. Harman, T.E. Higgins, S.L. Hodges, S.C. Hyde, L. Hyndman, J.A. Innes, J. Jacob, N. Jones, B.F. Keogh, M.P. Limberis, P. Lloyd-Evans, A.W. Maclean, M.C. Manvell, D. McCormick, M. McGovern, G. McLachlan, C. Meng, M.A. Montero, H. Milligan, L.J. Moyce, G.D. Murray, A.G. Nicholson, T. Osadolor, J. Parra-Leiton, D.J. Porteous, I.A. Pringle, E.K. Punch, K.M. Pytel, A.L. Quittner, G. Rivellini, C.J. Saunders, R.K. Scheule, S. Sheard, N.J. Simmonds, K. Smith, S.N. Smith, N. Soussi, S. Soussi, E.J. Spearing, B.J. Stevenson, S.G. Sumner-Jones, M. Turkkila, R.P. Ureta, M.D. Waller, M.Y. Wasowicz, J.M. Wilson, P. Wolstenholme-Hogg, Repeated nebulisation of non-viral CFTR gene therapy in patients with cystic fibrosis: a randomised, double-blind, placebo-controlled, phase 2b trial, Lancet Respir. Med. 3 (2015) 684–691, https://doi.org/10.1016/S2213-2600(15)00245-3.

[2] U. Griesenbach, K.M. Pytel, E.W.F.W. Alton, Cystic fibrosis gene therapy in the UK and elsewhere, Hum. Gene Ther. 26 (2015) 266–275, https://doi.org/10.1089/hum.2015.027.

[3] A. Aartsma-Rus, A.M. Krieg, FDA approves Eteplirsen for Duchenne muscular dystrophy: the next chapter in the Eteplirsen Saga, Nucleic Acid Ther. 27 (2017) 1–3, https://doi.org/10.1089/nat.2016.0657.

[4] R.S. Finkel, E. Mercuri, B.T. Darras, A.M. Connolly, N.L. Kuntz, J. Kirschner, C.A. Chiriboga, K. Saito, L. Servais, E. Tizzano, H. Topaloglu, M. Tulinius, J. Montes, A.M. Glanzman, K. Bishop, Z.J. Zhong, S. Gheuens, C.F. Bennett, E. Schneider, W. Farwell, D.C. De Vivo, Nusinersen versus sham control in infantile-onset spinal muscular atrophy, N. Engl. J. Med. 377 (2017) 1723–1732, https://doi.org/10.1056/NEJMoa1702752.

[5] S.A. Moschos, M. Frick, B. Taylor, P. Turnpenny, H. Graves, K.G. Spink, K. Brady, D. Lamb, D. Collins, T.D. Rockel, M. Weber, O. Lazari, L. Perez-Tosar, S.A. Fancy, C. Lapthorn, M.X. Green, S. Evans, M. Selby, G. Jones, L. Jones, S. Kearney, H. Mechiche, D. Gikunju, R. Subramanian, E. Uhlmann, M. Jurk, J. Vollmer, G. Ciaramella, M. Yeadon, Uptake, efficacy, and systemic distribution of naked, inhaled short interfering RNA (siRNA) and locked nucleic acid (LNA) antisense, Mol. Ther. 19 (2011) 2163–2168, https://doi.org/10.1038/mt.2011.206.

[6] P. Sazani, F. Gemignani, S.H. Kang, M.A. Maier, M. Manoharan, M. Persmark, D. Bortner, R. Kole, Systemically delivered antisense oligomers upregulate gene expression in mouse tissues, Nat. Biotechnol. 20 (2002) 1228–1233, https://doi.org/10.1038/nbt759.

[7] S. Gao, F. Dagnaes-Hansen, E.J.B. Nielsen, J. Wengel, F. Besenbacher, K.A. Howard, J. Kjems, The effect of chemical modification and nanoparticle formulation on stability and biodistribution of siRNA in mice, Mol. Ther. 17 (2009) 1225–1233, https://doi.org/10.1038/mt.2009.91.

[8] J.V. Aukunuru, S.P. Ayalasomayajula, U.B. Kompella, Nanoparticle formulation enhances the delivery and activity of a vascular endothelial growth factor antisense oligonucleotide in human retinal pigment epithelial cells, J. Pharm. Pharmacol. 55 (2003) 1199–1206, https://doi.org/10.1211/0022357021701.

[9] D.M. Lynn, R. Langer, Degradable poly (beta-amino esters): synthesis, characterization, and self-assembly with plasmid DNA, J. Am. Chem. Soc. 122 (2000) 10761–10768, https://doi.org/10.1021/ja0015388.

[10] S.R. Little, D.M. Lynn, S.V. Puram, R. Langer, Formulation and characterization of poly (?? Amino ester) microparticles for genetic vaccine delivery, J. Control. Release 107 (2005) 449–462, https://doi.org/10.1016/j.jconrel.2005.04.022.

[11] R.J. Fields, C.J. Cheng, E. Quijano, C. Weller, N. Kristofik, N. Duong, C. Hoimes, M.E. Egan, W.M. Saltzman, Surface modified poly(?? Amino ester)-containing nanoparticles for plasmid DNA delivery, J. Control. Release 164 (2012) 41–48, https://doi.org/10.1016/j.jconrel.2012.09.020.

[12] N.A. McNeer, K. Anandalingam, R.J. Fields, C. Caputo, S. Kopic, A. Gupta, E. Quijano, L. Polikoff, Y. Kong, R. Bahal, J.P. Geibel, P.M. Glazer, W. Mark Saltzman, M.E. Egan, Nanoparticles that deliver triplex-forming peptide nucleic acid molecules correct F508del CFTR in airway epithelium, Nat. Commun. 6 (2015) 1–11, https://doi.org/10.1038/ncomms7952.

[13] R.J. Fields, E. Quijano, N.A. Mcneer, C. Caputo, R. Bahal, K. Anandalingam, M.E. Egan, P.M. Glazer, W.M. Saltzman, Modified poly(lactic-co-glycolic acid) nanoparticles for enhanced cellular uptake and gene editing in the lung, Adv. Healthc. Mater. 4 (2015) 361–366, https://doi.org/10.1002/adhm.201400355.

[14] S. Rahimian, M.F. Fransen, J.W. Kleinovink, J.R. Christensen, M. Amidi, W.E. Hennink, F. Ossendorp, Polymeric nanoparticles for co-delivery of synthetic long peptide antigen and poly IC as therapeutic cancer vaccine formulation, J. Control. Release 203 (2015) 16–22, https://doi.org/10.1016/j.jconrel.2015.02.006.

[15] P. Sazani, S.H. Kang, M.A. Maier, C. Wei, J. Dillman, J. Summerton, M. Manoharan, R. Kole, Nuclear antisense effects of neutral, anionic and cationic oligonucleotide analogs, Nucleic Acids Res. 29 (2001) 3965–3974, https://doi.org/10.1093/nar/29.19.3965.

[16] S.H. Kang, M.J. Cho, R. Kole, Up-regulation of luciferase gene expression with antisense oligonucleotides: implications and applications in functional assay development, Biochemistry. 37 (1998) 6235–6239, https://doi.org/10.1021/bi980300h.

[17] R. Bahal, N.A. McNeer, D.H. Ly, W.M. Saltzman, P.M. Glazer, Nanoparticle for delivery of antisense gammaPNA oligomers targeting CCR5, Artif DNA PNA XNA. 4 (2013) 49–57, https://doi.org/10.4161/adna.25628.

[18] R. Bahal, E. Quijano, N.A. McNeer, Y. Liu, D.C. Bhunia, F. Lopez-Giraldez, R.J. Fields, W.M. Saltzman, D.H. Ly, P.M. Glazer, Single-stranded γPNAs for in vivo site-specific genome editing via Watson-crick recognition, Curr. Gene Ther. 14 (2014) 331–342, https://doi.org/10.1016/j.jsbmb.2011.07.002.Identification.

[19] R. Bahal, N. Ali McNeer, E. Quijano, Y. Liu, P. Sulkowski, A. Turchick, Y.C. Lu, D.C. Bhunia, A. Manna, D.L. Greiner, M.A. Brehm, C.J. Cheng, F. López-Giráldez,

A. Ricciardi, J. Beloor, D.S. Krause, P. Kumar, P.G. Gallagher, D.T. Braddock, W. Mark Saltzman, D.H. Ly, P.M. Glazer, In vivo correction of anaemia in β-thalassemic mice by γ3PNA-mediated gene editing with nanoparticle delivery, Nat. Commun. 7 (2016), https://doi.org/10.1038/ncomms13304.

[20] N.A. McNeer, J.Y. Chin, E.B. Schleifman, R.J. Fields, P.M. Glazer, W.M. Saltzman, Nanoparticles deliver triplex-forming PNAs for site-specific genomic recombination in CD34+ human hematopoietic progenitors, Mol. Ther. 19 (2011) 172–180, https://doi.org/10.1038/mt.2010.200.

[21] I.A. Babar, C.J. Cheng, C.J. Booth, X. Liang, J.B. Weidhaas, W.M. Saltzman, F.J. Slack, Nanoparticle-based therapy in an in vivo microRNA-155 (miR-155)-dependent mouse model of lymphoma, Proc. Natl. Acad. Sci. 109 (2012) E1695–E1704, https://doi.org/10.1073/pnas.1201516109.

[22] A.H. Ghassemi, M.J. van Steenbergen, H. Talsma, C.F. van Nostrum, W. Jiskoot, D.J.A. Crommelin, W.E. Hennink, Preparation and characterization of protein loaded microspheres based on a hydroxylated aliphatic polyester, poly(lactic-co-hydroxymethyl glycolic acid), J. Control. Release 138 (2009) 57–63, https://doi.org/10.1016/j.jconrel.2009.04.025.

[23] E.V.B. van Gaal, R.S. Oosting, W.E. Hennink, D.J.A. Crommelin, E. Mastrobattista, Junk DNA enhances pEI-based non-viral gene delivery, Int. J. Pharm. 390 (2010) 76–83, https://doi.org/10.1016/j.ijpharm.2009.08.032.

[24] H. Gao, W. Shi, L.B. Freund, Mechanics of receptor-mediated endocytosis, Proc. Natl. Acad. Sci. U. S. A. 102 (2005) 9469–9474, https://doi.org/10.1073/pnas.0503879102.

[25] S. Zhang, J. Li, G. Lykotrafitis, G. Bao, S. Suresh, Size-dependent endocytosis of nanoparticles, Adv. Mater. 21 (2009) 419–424, https://doi.org/10.1002/adma.200801393.

[26] A.W. Barrios, G. Núñez, P. Sánchez Quinteiro, I. Salazar, Anatomy, histochemistry, and immunohistochemistry of the olfactory subsystems in mice, Front. Neuroanat. 8 (2014), https://doi.org/10.3389/fnana.2014.00063.